ELSEVIER

Spectrochimica Acta Part A 53 (1997) 2627–2639

SPECTROCHIMICA ACTA PART A

Ni/sepiolite hydrogenation catalysts Part 1: Precursor–support interaction and nature of exposed metal surfaces

James A. Anderson *, Sarah E. Falconer, Mercedes Galán-Fereres

Department of Chemistry, University of Dundee, Dundee, DD1 4HN, UK

Received 6 May 1997; received in revised form 25 July 1997; accepted 31 July 1997

Abstract

A 10% loaded nickel on sepiolite catalyst has been prepared by a precipitation method and the characteristics of the resultant material compared with a similarly prepared Ni/silica catalyst and a sample in which only ion exchanged nickel was present in the sepiolite. Samples have been characterised by infrared (IR) and X-ray photoelectron spectroscopies, ^{29}Si MAS–NMR and X-ray diffraction in an attempt to determine the nature of the nickel species present in the precursor stage. Nickel silicate species have been identified for both supports but this precursor is more resistant to reduction for the sepiolite which leads to the formation of catalysts with lower metal areas than the silica support. The nature of the reduced nickel particles has been determined by hydrogen chemisorption, IR of adsorbed CO and temperature programmed desorption of hydrogen. © 1997 Elsevier Science B.V.

Keywords: Nickel catalyst; Sepiolite; Precursor-support interaction

1. Introduction

Nickel/silica catalysts have been widely studied due to their importance in hydrogenation reactions [1], in particular hydrogenation of olefins [2] and natural oils [3,4]. Catalysts' properties are known to be influenced by preparation procedures and the influence of preparation variables has received attention [5–7]. Although normally considered an inert carrier, it is known that under certain conditions, strong interactions between the Ni precursor and the silica surface exist [4,8], which leads to difficult-to-reduce nickel species [9–11] and active catalysts, which contain a proportion of unreduced nickel [4,5]. This is the case, particularly, where precipitation procedures have been involved [4,8,9,11,12].

Natural silicate materials have also been studied as supports for nickel hydrogenation catalysts [13–16]. As observed for Ni/silica catalysts, com-

* Corresponding author. Tel.: +44 382 23181; fax: +44 382 201604.

PII S1386-1425(97)00197-2

plete reduction to the metal is seldom achieved, even for high reduction temperatures [13–16]. In a recent study, the hydrogenation of benzene and styrene over Ni/sepiolite catalysts was investigated for samples prepared by impregnation and precipitation procedures [15,16]. The two series of samples showed differences in catalytic behaviour over a range of dispersions. IR results indicated that differences in particle morphology existed between the two series of catalysts. Although blockage of certain planes or sites [7,17] or preferential exposure of certain crystal faces would give a possible explanation of results, the role of unreduced nickel species was considered to play an important role. Catalysts which exhibited the lowest activity per exposed nickel atom in benzene hydrogenation proved to be the most active in styrene hydrogenation, and were those catalysts which showed a high level of unreduced surface nickel. Styrene was proposed to adsorb via the ethylene double bond at incompletely-reduced nickel sites, whereas ensembles of reduced nickel atoms were required to allow planar adsorption as a prerequisite for benzene hydrogenation or for the non-selective hydrogenation of styrene to ethylcyclohexane.

In order to ascertain whether unreduced nickel may play a role in the hydrogenation behaviour of these catalysts, the adsorptions of styrene and benzene have been investigated using surfaces which are rich in Ni^{2+} sites and on a catalyst where the exposed nickel is mainly reduced. In order to overcome the limitations of IR spectroscopy—mainly high absorption in the low frequency region and loss of features due to the surface selection rule—vibrational spectra have been obtained using inelastic neutron scattering (INS). The results of the INS study will be presented in a following paper [18]. In this paper we report characterisation details of the sample used in the INS measurements using in situ pretreatments akin to those carried out prior to exposure to the adsorbates in the INS cell. A similarly prepared Ni/silica catalyst has been used to determine whether the interactions between metal and support are of a similar nature for silica and silicate materials.

2. Experimental

2.1. Catalyst preparation

The sepiolite (Yunclillos, Toledo, Spain, $>95\%$ pure) and silica (Aerosil 200 Degussa) were used as supplied. Catalysts were prepared by a precipitation method [12] by firstly adding a solution of nickel nitrate to a suspension of the support material and adjusting the pH to 3.5 by the addition of nitric acid. This was heated to 363 K before addition of a urea solution which resulted in the controlled precipitation of hydroxide over the support. After 48 h, the suspension was filtered, and the precipitate repeatedly washed with distilled water. Samples were dried at 383 K in air for 16 h and then treated firstly in a N_2 flow (100 $cm^3\ min^{-1}$) at 573 K for 3 h and then in a 3.5%H_2 in Ar flow (100 $cm^3\ min^{-1}$) at 773 K for 5.5 h before cooling to ambient temperature in a flow of N_2.

2.2. Characterisation methods

In general, characterisation was carried out over the high temperature (773 K) prereduced sample which was passivated and then either outgassed in situ at 393 K or re-reduced at 673 K. Additional experiments were carried out directly on the dried precursor material.

IR spectra were recorded as an average of 100 scans (resolution of 4 cm^{-1}) using a Perkin Elmer 1720X FT spectrometer fitted with TGS detector and connected to a Perkin Elmer 7300 computer or PC. Self supporting wafers of 25 mm diameter were located in a high vacuum system fitted with an external furnace and CaF_2 windows allowing sample pretreatment to be conducted in situ. These were reduced in a flow (100 $cm^3\ min^{-1}$) of H_2 (3.5% v/v) in Ar by raising the temperature by 5 K min^{-1} to 673 K and then maintaining this temperature for 1 h. The cell was evacuated for 10 min with the sample at the elevated temperature, before cooling to ambient temperature in dynamic vacuum. Samples were exposed to CO pressures of between 1 and 20 torr and then the CO removed by evacuation at ambient temperature for periods of between 30 s and 10 min. Spectra are

presented by subtraction of a background spectrum, recorded after sample pretreatment but prior to exposure to CO. Spectra in the 1100–500 cm^{-1} range were obtained using $\approx 5\%$ of sample in KBr discs. Spectra in the OH stretching region (3800–3400 cm^{-1}) were obtained in the diffuse reflectance mode with the sample contained within a Harrick DRIFT environmental chamber. Previously unreduced samples were heated under vacuum to 573 K and then held at this temperature for 1 h or heated in a flow of H_2 in Ar from ambient temperature up to 773 K, maintaining the temperature at each elevated value for sufficient time to allow recording of the spectrum.

^{29}Si NMR (59.6 MHz) spectra of the materials were obtained using a chemagnetics multinuclear FT spectrometer. Powdered samples were contained within 7.5 mm diameter zirconia rotors and spun using compressed air at 5 kHz at an angle of 54° 44' to the magnetic field. One-pulse experiments were conducted using a pulse width of 4 μs and a 10 s delay. This delay was chosen following saturation recovery experiments which indicate T_1 to be of the order of 1 s. Up to 3500 acquisitions were made. Instrument calibration was performed using 3(trimethylsilyl)-1-propanesulphonic acid sodium salt.

Nickel dispersion and particle size were calculated from hydrogen adsorption isotherms measured at 298 K and also from hydrogen temperature programmed desorption (TPD) analysis performed using an Altamira AMI-1 catalyst characterisation system. For these experiments, samples were re-reduced in situ by heating in a flow of H_2 (100 cm^3 min^{-1}) at 673 K for 1 h. The system was purged with Ar for 15 min at 303 K to remove gaseous and physisorbed hydrogen before monitoring desorbed hydrogen while heating at 10 K min^{-1} to 823 K. The analysis was repeated four times using a fresh sample each time. Static measurements were performed using similarly pretreated samples but then outgassing at 673 K for 30 min prior to exposure to hydrogen at 298 K.

The quantity of unreduced nickel remaining in the 773 K reduced sample following re-reduction in situ at 673 K was calculated gravimetrically using a Sartorius 4102 microbalance. Samples were re-oxidised by heating in a flow of O_2 (50 cm^3 min^{-1}) at 10 K min^{-1} to 673 K and then maintaining this temperature for 1 h. The apparatus was then flushed briefly in nitrogen before introducing a flow of H_2 (100 cm^3 min^{-1}) and measuring the weight loss due to reduction at 673 K as a function of time.

BET surface areas were measured on a Micromeritics model 2205 surface area analyser from single point analysis using Ar as adsorbate on samples pretreated in flowing Ar at 423 K.

3. Results

Table 1 lists BET surface areas of the supports and catalysts. Incorporation of nickel in each case leads to some loss of area for both support materials, although the effect is most pronounced for silica. Reduction of the catalysts at 773 K leads to further loss of area, although the supports alone under similar thermal treatments show an equivalent loss.

Fig. 1 shows spectra of the catalysts in KBr discs. Samples of Ni/silica after drying but prior to reduction (Fig. 1A(b)), show a doublet at 670/661 cm^{-1} not observed for silica alone (Fig. 1A(a)) in addition to the band at 806 cm^{-1} and a weak shoulder at ≈ 900 cm^{-1} present for both. The 806 cm^{-1} band is due to an O–Si–O symmetric stretching mode of the silica, whereas the 670/661 cm^{-1} doublet is clearly related to the nickel precursor as shown by the depleted inten-

Table 1
BET (Ar) surface areas for sepiolite and silica supports and 10% Ni catalysts

Sample	Pretreatment	BET surface area (m^2 g^{-1})
Sepiolite	Dried 423 K	135
	Reduced 773 K	119
Ni ion exc sepiolite	Dried 423 K	125
10% Ni/sepiolite	Dried 423 K	112
	Reduced 773 K	110
Silica Aerosil 200	Dried 423 K	179
10% Ni/Silica	Dried 423 K	140
	Reduced 773 K	116

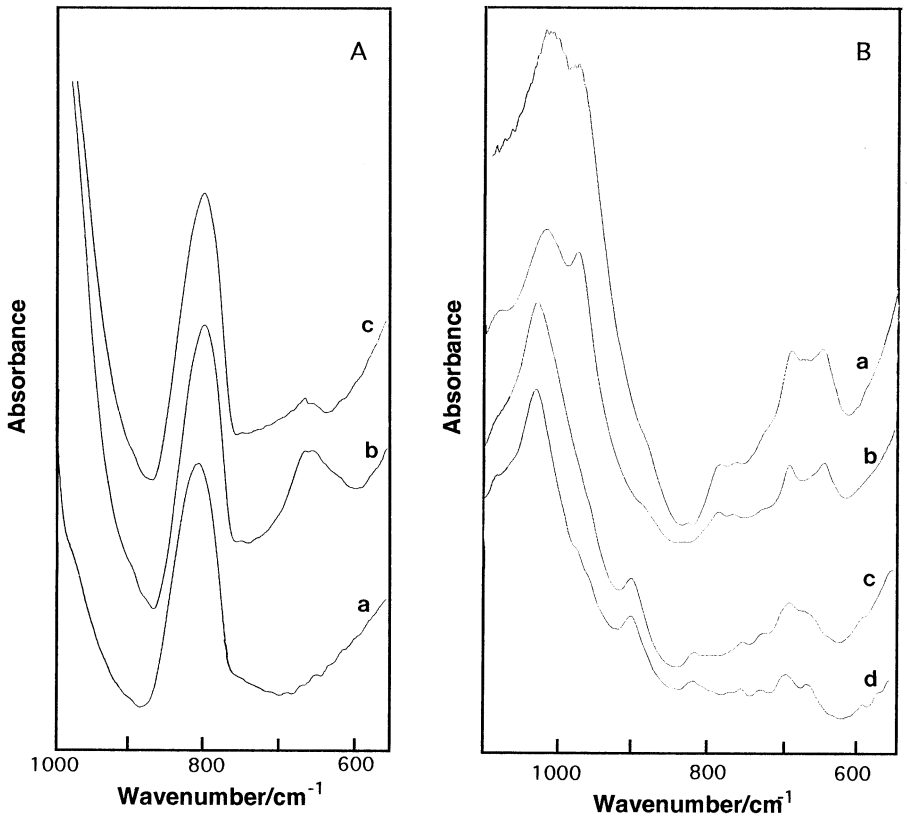

Fig. 1. A, IR spectra of (a) silica, (b) Ni/silica dried at 383 K and (c) Ni/silica reduced at 773 K. B, IR spectra of (a) Ni/sepiolite dried at 383 K, (b) sepiolite dried at 383 K (c) Ni/sepiolite reduced at 773 K and (d) sepiolite reduced at 773 K.

sity of the feature following reduction at 773 K. No three-dimensional structures were detected of the nickel precursor by powder X-ray diffraction.

Fig. 1B compares bands in the low frequency region for dried and reduced Ni/sepiolite with similarly pretreated samples of the support. The band at 1032 cm^{-1}, present for both catalyst and support, is centred at 1005 cm^{-1} for the samples which were not treated at high temperature. The 773 K treatment essentially removes the species responsible for the band at 980 cm^{-1} and allows the band at 902 cm^{-1} to be resolved. The other features which were observed were all of lesser intensity, with the most important being found at 692/669 cm^{-1} for the 773 K reduced sepiolite and Ni/sepiolite samples (Fig. 1B(c,d)) and at 783/762 and 687/648 cm^{-1} in the case of the dried samples (Fig. 1B(a,b)). The latter doublet appeared to be better resolved for the sepiolite alone, probably due to the presence of an additional component at ≈ 670 cm^{-1} for the dried Ni/sepiolite (Fig. 1B(a)). Under the same conditions in the O–H stretching region (not shown), maxima at 3631(sh), 3560, 3404 and 3262 cm^{-1} were observed for the 383 K dried, unreduced catalyst.

To obtain further information from the O–H stretching region, DRIFT spectra were recorded following outgassing at 573 K to remove much of the physisorbed water. The main features of the spectrum are bands at 3733, 3712, 3685, 3672, 3603, 3593, and 3528 cm^{-1} (Fig. 2(a)). Under similar conditions, the main features for the Ni/sepiolite precursor were maxima at 3672, 3644, 3617, 3603(sh), 3593 and 3528 cm^{-1} (Fig. 2(b)).

The ^{29}Si MAS–NMR spectrum of sepiolite shows three main lines at -92, -95 and -98

ppm (Fig. 3(a)) in agreement with previous studies [19–21] and as expected for a structure where the tetrahedral layer exhibits inversion at every sixth silicon, giving rise to three different sites (centre, near edge and edge) of similar concentrations. In further agreeement [19–21], an additional weaker line at -85 ppm was observed. This feature was not observed under similar conditions for a sample of the Ni/sepiolite prior to reduction (Fig. 3(b)). Additionally, the sample containing the nickel precursor exhibited poorer resolution between the three main lines, part of which might be attributed to the appearance of an additional component at ≈ -93.5 ppm. However, when deconvolution techniques were applied to the spectra, it was found that a three-component fit could be used to adequately account for both spectra in the -90 to -105 ppm region, with enhanced line width for the Ni containing sample

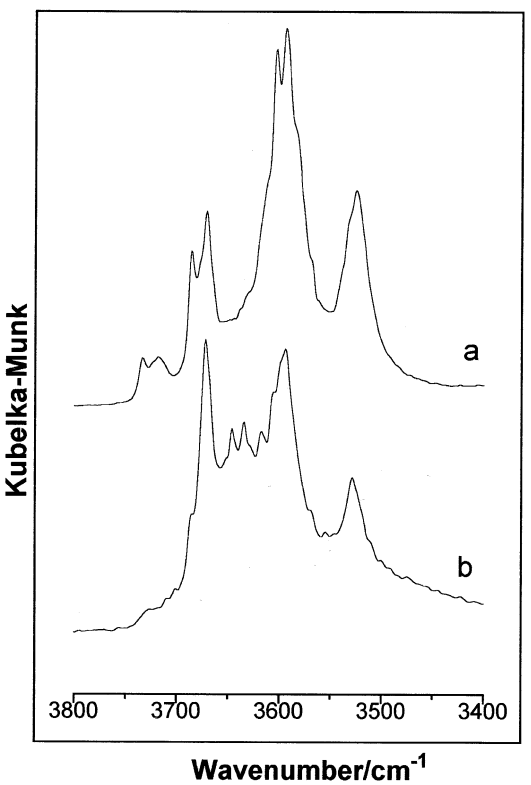

Fig. 2. DRIFT spectra of (a) sepiolite and (b) Ni/sepiolite precursor following outgassing in situ at 573 K for 1 h.

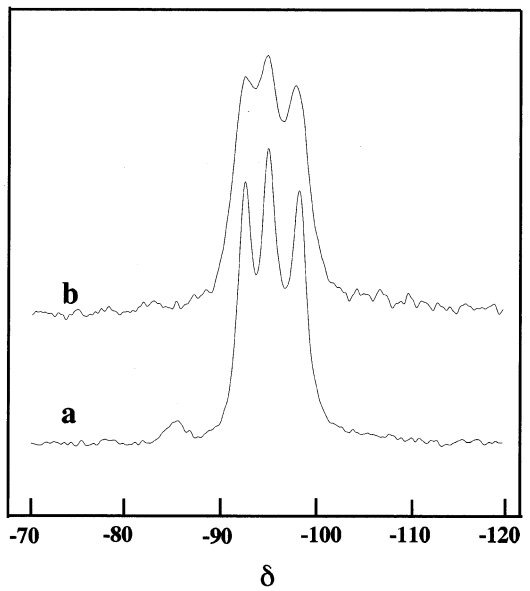

Fig. 3. One-pulse ^{29}Si MAS–NMR spectra of (a) sepiolite and (b) unreduced Ni/sepiolite.

accounting for the loss in resolution between the components.

To determine how the hydroxyl species, and in particular those which might be related to the nickel precursor, were affected during the reduction procedure, some dried, unreduced sample was heated in a flow of H_2 in Ar and spectra collected at 100 K intervals up to 773 K. Spectra of the Ni/sepiolite (Fig. 4B) are compared with those for a similarly pretreated nickel-free sample (Fig. 4A). Samples treated at 473 K still contained molecular water within the sepiolite channels resulting in high absorption of radiation by the sample and leading to a high level of noise in the spectra recorded. At 573 K the spectrum of sepiolite (Fig. 4A(b)) resembled the 573 K outgassed sample (Fig. 2(a)). By 773 K, the main spectral features for sepiolite were bands at 3733/3712, 3672, 3593 and 3525 cm^{-1} (Fig. 4A(d)), whereas at the same temperature the Ni/sepiolite showed maxima at 3672, 3644 and 3593 cm^{-1} (Fig. 4B(d)).

Fig. 5 shows spectra of CO adsorbed on the prereduced catalyst which was subsequently passivated and then outgassed in situ at 393 K. The

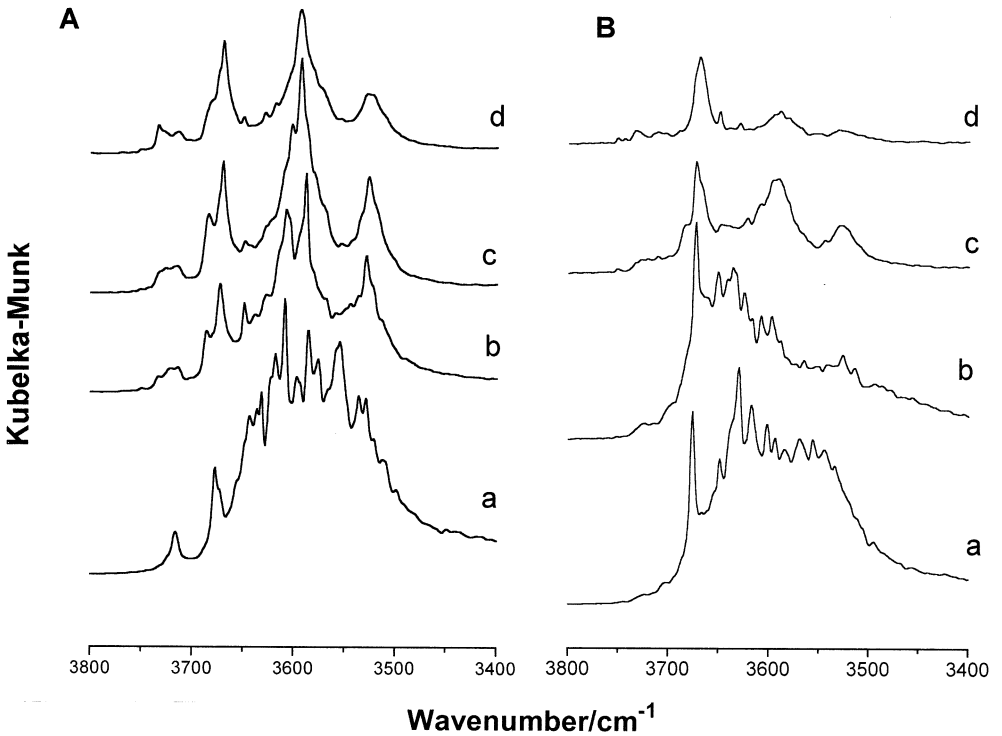

Fig. 4. DRIFT spectra of A, sepiolite and B, Ni/sepiolite precursor heated in H_2/Ar with spectra recorded at (a) 473, (b) 573, (c) 673 and (d) 773 K.

absence of bands below 2100 cm^{-1} indicates that no Ni^0 atoms are exposed at the catalyst surface following the outgassing treatment and that the reduced metal particles probably contain a film of oxide with an outer layer of O^{2-} ions or a layer of chemisorbed oxygen atoms. The band at 2196 cm^{-1} with a shoulder at 2185 cm^{-1} indicates the presence of Ni^{2+} centres [14–16,22]. In accordance with the weak interaction with Ni^{2+}, CO was almost completely removed by brief evacuation at 298 K (Fig. 5(1b)). Ni^{2+} sites were also detected by CO in a sample where nickel had been introduced by ion-exchange. The sample outgassed in situ at 393 K gave a band at 2196 cm^{-1} with slight asymmetry (2185 cm^{-1}) towards lower frequency (Fig. 5(2a)). The adsorbate was almost completely removed by brief evacuation. A sample of nickel-free sepiolite, treated in a similar manner, gave no evidence of adsorption (Fig. 5(3a)) confirming that the band at 2196 cm^{-1} can be attributed to exposed nickel cations in the structure.

X-ray photoelectron spectroscopies (XPS) of the prereduced 10% Ni/sepiolite sample, outgassed in situ for 1 h at 393 K, showed two main features in the Ni($2p_{3/2}$) region corresponding to binding energies of 869.3 and 857.6 eV. The former is due to the Ni^{2+} shake up satellite. The latter could be deconvoluted to give two components with the smaller contribution corresponding to a binding energy of 855.0 eV indicating Ni^0. The contribution of Ni^0 to the total nickel signal (including the Ni^{2+} satellite peak) was calculated to be 0.08.

The bulk of the remainder of experiments were performed on samples which were re-reduced in situ at 673 K within the appropriate apparatus. Fig. 6 shows IR spectra of CO adsorbed on reduced samples. The 10% Ni/sepiolite sample following re-reduction at 673 K and exposure to

20 torr CO (Fig. 6(b)) showed features at 2196, 2175(sh), 2139, 2096, 2084(sh), 2066(sh), 2012, 1956 and 1945(sh). Evacuation for 5 min at 298 K allowed several of the features to be more clearly observed, and allowed identification of additional bands at 2125, 1995(sh), 1985(sh) and 1904 cm^{-1} (Fig. 6(c)). Curiously, the band at 2196 cm^{-1}, already assigned to CO adsorbed at exposed Ni^{2+} sites, was still observed after evacuation for 5 min, whereas similar species were readily removed from a surface outgassed at 393 K.

In order to investigate the reducibility of the nickel species, samples were reduced for 2 h at 873 K in the IR cell. Exposure to CO gave the spectrum in Fig. 6(a), with bands at 2196, 2139, 2096(sh), 2063, 2022(sh), 2015, and 2053 cm^{-1}. The additional thermal treatment involved in almost eliminating Ni^{2+} sites from the surface, clearly results in considerable modifications to the metallic nickel crystallites. The spectrum of the high temperature treated Ni/sepiolite bears a closer resemblance to the 673 K in situ reduced Ni/silica sample (previously reduced at 773 K) where maxima at 2080(sh), 2058, 2030(sh) and ≈ 1950 cm^{-1} were observed (Fig. 6(d)) with no evidence for surface Ni^{2+} species.

Samples re-reduced at 673 K in situ in the XPS chamber showed similar features to the 393 K outgassed samples, although differing in fine detail. The two main peaks were apparent at 869.3 and 857.5 eV with deconvolution of the latter indicating a binding energy of 854.0 eV for the Ni^0 species. This peak represented only 0.05 of the total nickel signal, and a decrease in the nickel/silicon ratio from 3.93 to 3.52 from in situ outgassing at 393 K to in situ reduction at 673 K,

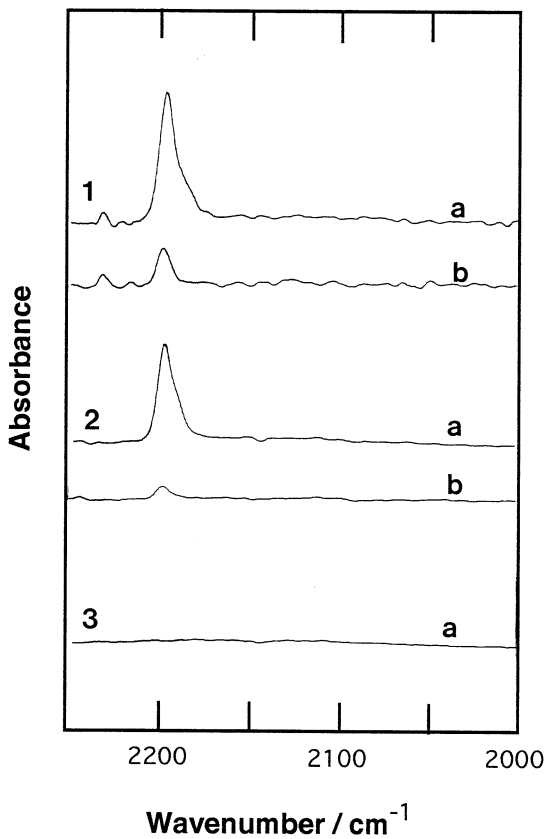

Fig. 5. IR spectra of (1) 10% Ni/sepiolite (prereduced at 773 K, 5 h), (2) Ni ion-exchanged sepiolite, and (3) sepiolite, all out-gassed in situ at 393 K prior to (a) exposure to 10 torr CO and (b) evacuation at 298 K for 30 s.

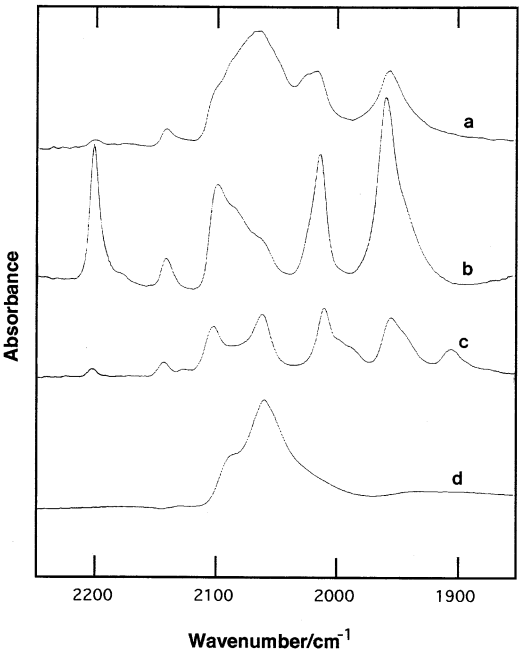

Fig. 6. IR spectra of prereduced (773 K, 5 h) catalysts exposed to 20 torr CO at 298 K (a) Ni/sepiolite reduced in situ at 873 K for 2 h, (b) Ni/sepiolite reduced in situ at 673 K for 1 h and (c) evacuation for 5 mins after exposure to CO, and (d) Ni/SiO_2 reduced in situ at 673 K for 1 h.

Table 2
Catalyst characteristics

Catalyst	Ni (%)	Metal area (m^2 g^{-1} Ni)	Degree of reduction	Dispersion (%)	Particle size (nm)
Ni/silica					
(T_R 673)	10.0	134.6	0.95	20.3	3.8
Ni/sepiolite	10.0	[162.5]	0.58	[40.2]	[1.94]
(T_R 673)		42.4		10.5	7.4
(T_R 873)		50.6	0.95	7.6	10.2

From hydrogen isotherms at 298 K and [ ] values calculated from hydrogen TPD.
[a] T_R refers to the temperature of the in situ reduction temperature performed on samples previousy reduced at 773 K.

indicates some loss in dispersion during the latter treatment.

Hydrogen TPD on the Ni/sepiolite sample gave a positive detector response over the range 323–923 K with three distinct maxima at 355–359, 689–706 and 815–848 K. From Table 2 it can be seen that dispersion calculations made using this data overestimate the amount of exposed nickel, probably as a result of inclusion of the desorption peak at 815–848 K, above the maximum pretreatment temperature and probably resulting from hydrogen desorption from the support. Ni/silica samples gave higher metal areas than similarly pretreated Ni/sepiolite, mainly as a result of a higher degree of reduction. However, even accounting for the unreduced nickel present, the silica supported sample gave the higher dispersion. Increasing the reduction temperature to 873 K increased the total metal area as a result of the higher degree of reduction, but this lead to a decrease in the total dispersion.

4. Discussion

4.1. Nature of the nickel precursor: silica support

The high temperature (773 K) chosen to reduce the nickel to the metallic state was instigated by the known strong interaction between precursor and silica surface [4–12]. Although studies continue with the objective of determining the exact nature of the supported phases formed during the preparation [23], there is general agreement that nickel silicates are formed at the surface [5,8–12,23]. The absence of an XRD pattern for NiO, which was observed for an equivalent loading of Ni on silica produced by impregnation and the detection of IR bands in the 600–750 cm^{-1} region (Fig. 1A), suggest that surface phyllosilicates (lamellar silicates) may have been formed. Careful analysis of this region of the IR spectrum may allow the phyllosilicates to be distinguished from nickel hydroxides and oxyhydroxides and may allow discrimination between different phyllosilicates (e.g. 2:1 and 1:1 structures) [23–26]. Layer silicates exhibit bands in the 950–600 cm^{-1} region due to O–H bending modes and between 1200–700 cm^{-1} due to Si–O stretching vibrations [24]. The δ_{O-H} band for $Ni(OH)_2$ is sensitive to the degree of crystallisation and the presence of interlamellar water and gives a band between 520–640 cm^{-1} whereas the same mode for the nickel phyllosilicate is less sensitive and gives a band at ≈ 670 cm^{-1} [23]. As long as the amount of water intercalated between layers is not so great as to inhibit its observation, Ni talc (2:1) gives rise to two bands in this region at 711 cm^{-1} due to δ_{O-H} and at ≈ 665 cm^{-1} due to superimposition of δ_{O-H} and ν_{Si-O} modes while nepouite (1:1) always give a single maximum at ≈ 665 cm^{-1} [23,26]. From the spectra recorded here, giving a single band at ≈ 665 cm^{-1} with two features at 670/661 cm^{-1} (Fig. 1A(b)), it would appear that mainly Ni phyllosilicate rather than hydroxide has been formed and that this has a nepouite rather than talc-like structure. The presence of a tail on the band towards 620 cm^{-1} may indicate the presence of some poorly crystalline $Ni(OH)_2$ which would be consistent with previous

results where both hydroxide and nepouite were identified following a similar preparation procedure [23].

Even after reduction at 773 K, some evidence for the nickel silicate structure remains (Fig. 1A(c)). Coenen [4] has suggested that some of the Ni–O–Si linkages of the nickel silicates remain following reduction and that these unreduced nickel species are located at the interface between the support and the hemispherical nickel particles formed. As no band at 2200 cm^{-1} was observed for CO adsorbed on the reduced catalyst (Fig. 6(d)), despite the detection of residual nickel silicate by IR (Fig. 1A(c)) and the incomplete degree of reduction measured gravimetrically (Table 2), it may be that the inaccessible Ni^{2+} is located in these environments.

4.2. Nature of the nickel precursor: sepiolite support

We have previously demonstrated that the above model [4], however, does not hold for nickel/silicate catalysts from the shape of degree of reduction/particle size plots [15] and the detection of surface Ni^{2+} species by probing with CO [14–16]. Similarly here, the detection of IR bands at 2196 and 2185 cm^{-1} for the in situ reduced Ni/sepiolite confirm the accessibility, and hence surface nature of such species. Although a proportion of these Ni^{2+} sites are produced by exchanging Mg^{2+} for Ni^{2+}, as confirmed by detection of similar bands in the spectra of CO adsorbed on the ion-exchanged sample (Fig. 5(2)), the degree of reduction experiments confirm that the quantity of nickel remaining in an unreduced state (4.2% wt) is far greater than the quantity which can be incorporated into the support structure via exchange (5–12 mEq/100 g) [21]. Atomic absorption measurements indicate this to be 1.09% wt for the sample prepared here.

The nature of this nickel phase may be deduced from differences between dried and reduced catalysts when compared with the nickel free sepiolite spectra (Fig. 1). Bands at 1032 and 692 cm^{-1} compare with those at 1039 and 687 cm^{-1} for Mg talc which can be accounted for by the vibrations expected for an ideal hexagonal $(Si_2O_5)_n$ layer [24]. Similarly the 669 cm^{-1} band compares with a similar feature in Mg talc due to the δ_{O-H} [24]. In previous studies where nickel was precipitated onto silicate surfaces, the 1:1 type nickel hydrosilicate, antigorite $[Ni_2(OH)_4Si_2O_5]$ was proposed as the precursor formed [14,27]. Additional features in the spectrum of the dried Ni/sepiolite (Fig. 1B(a)) at 1080, 980 and 648 cm^{-1} are in good agreement (1078, 994/969, 646 cm^{-1}) with the antigorite spectrum [24] but as these appear for sepiolite alone (Fig. 1B(b)) and are similarly affected by high temperature reduction as the Ni/sepiolite, it is unlikely that these bands are indicative of the Ni precursor phase. It is more likely that these differences between dried and high temperature reduced samples are related to the degree of hydration of the samples. Similarly, although Kermarec et al. [23] state that a Si–O vibration at 1005 cm^{-1} unambiguously characterises a nepouite-like phase, the detection of similar maxima for both the support and supported catalyst in their dried states indicate that the exact position of the Si–O band is influenced by the degree of hydration and may not be used as a characteristic of the precursor phase.

As indicated above, the main difference between the spectra of dried catalyst and support is the resolution between the 687/648 cm^{-1} pair, probably due to the presence of a band at ≈ 670 cm^{-1} for the former. As discussed above for the case of Ni/silica, the appearance of a maximum at 670 cm^{-1} in the absence of a band at 711 cm^{-1} would suggest [23,26] the presence of nickel in a nepouite- rather than talc-like structure.

Spectra in the O–H stretching region for the low temperature pretreated samples are rather more complex than the four band spectrum reported by Cannings [28], however, the four maxima correspond well with the observed features at 3733, 3672, 3603 and 3528 cm^{-1} (Figs. 2 and 4). The latter pair are assigned to the asymmetric and symmetric stretching modes of molecular water coordinated to Mg^{2+} ions at the edges of the channels [28]. These bands are absent following heating between 673 and 873 K [28], consistent with the known removal of water from these positions at ≈ 723 K [21]. This water appears to be more readily removed from the Ni/sepiolite

(Fig. 4B(d)) than from the nickel free sample (Fig. 4A(d)). The band at 3672 cm^{-1} observed for sepiolite [28–30] is also observed for antigorite and Mg talc [24] and assigned to hydroxyls on Mg^{2+} ions. Of greater interest are the bands at 3733 and 3712 cm^{-1}, probably due to free [28] and adjacent hydroxyls on silicon atoms, as these are clearly affected by the presence of the Ni precursor (Fig. 2(a,b) and 4A,B). These SiOH groups are produced when Si–O–Si bridges linking the silicate layers are broken, leaving terminal OH groups. From the chemical shift value observed (-85 ppm), it would appear that these are geminal (Q^2) rather than single silanols (Q^3). During the preparation procedure, the pH varies from <3.0 to ≈ 5.8. It is known that both acid [29] and basic [30] media may attack the sepiolite structure, although in both cases, an increase in the number of SiOH groups is expected as acid treatment leads to the extraction of Mg^{2+} ions from the silicate leading to formation of SiO_2 [13,29] and hydrolysis of the silicate structure occurs in basic media [30]. Precipitation–deposition of the nickel precursor appears to consume such hydroxyls.

The loss of SiOH groups by interaction between sepiolite and nickel precursor was confirmed by the loss of the -85 ppm line in the NMR spectrum (Fig. 3). Although there is some disagreement over the exact assignment [19,20], this line would appear to be due to an edge silicon atom bonded to hydroxyl, [19–21] probably Q^2(Si–OH) [19,21]. A reverse correlation between the -85 ppm line and the -98 ppm resonance, due to Si atoms at the edge of a silicate ribbon and bonded via a basal oxygen to an adjacent silicate layer [19] would confirm the assignment to a hydroxyl bound to an edge silicon.

The suppression of Si–OH species for the Ni/sepiolite precursor is compensated by additional bands at 3644 and 3634 cm^{-1} (Fig. 2(b)) which do not appear in the spectrum of the outgassed sepiolite alone. Similarly, although maxima appear in this region for sepiolite heated under reducing conditions (Fig. 4A), the relative intensities (compare for example Fig. 4A(b) and B(b)) are considerably greater in this spectral region for the nickel-containing sample, indicating additional types of hydroxyl groups to be present.

Ni talc and nepouite are expected to give bands due to ν_{O-H} at 3625 and 3645 cm^{-1}, respectively [26]. However, partial replacement of magnesium by nickel may give up to four stretching frequencies (3677, 3663, 3646 and 3627 cm^{-1}) corresponding to the possible combinations of the two different cations within the three octahedral sites which are directly linked to a hydroxyl group [24]. High degrees of substitution give rise to a single maximum at 3627 cm^{-1}, consistent with the expected value for Ni talc [26]. The band pair at 3644 and 3634 cm^{-1} observed for the Ni/sepiolite precursor may not be unambiguously assigned but probably indicate the presence of Ni substituted into the octahedral layer and Ni–OH in a nepouite type layer, the latter being consistent with the band assignment at 670 cm^{-1} to δ_{O-H} of a similar structure [24]. The presence of a nickel silicate would be consistent with the detection of an additional line at -93.5 ppm in the ^{29}Si NMR spectrum (Fig. 3(b)). However, as indicated above, the spectrum shape can be accounted for by line broadening without the need to include a forth component.

The assignment of the precursor species from IR data to a nickel silicate rather than $Ni(OH)_2$ is consistent with XPS analysis, where values for $Ni(2p_{3/2})$ satellite separation (ΔE_{sat}) of 5.9 and 5.8 eV (383 and 673 K treatments, respectively) correlate with a value of 6.0 eV for nickel silicate rather than 5.4 eV expected for $Ni(OH)_2$ [27].

These precursor species appear to undergo dehydration/decomposition/reduction between 573–673 K in accordance with the dramatic losses in the OH band intensity over this temperature range (Fig. 4B(b,c)), although evidence for their presence exist even at 773 K. This is completely consistent with the failure to obtain complete reduction at this temperature (Table 2) and the detection of surface Ni^{2+} by adsorption of CO (Fig. 6). Differences between the reducibility of the Ni/silica and Ni/sepiolite samples indicate differences in the exact nature of the silicates formed, which will be important in determining particle morphology and the nature of the exposed metal surfaces in the reduced catalysts.

4.3. Nature of exposed metal faces

IR spectra of CO adsorbed on nickel surfaces indicate the presence of three main adsorption modes which are characterised by bands at 2070–1950, 1950–1900 and 1900–1850 cm^{-1} due to linear, 2-fold and 3-fold bridging modes, respectively. In addition to these main features appearing on low index faces, bands appearing between 2100–2075 cm^{-1} for both sepiolite and silica supported nickel catalysts (Fig. 6) do not coincide with features detected on extended faces of single crystals. These can be attributed to linear adsorption on small particles where the high frequency position results from the metal–support interaction where a large number of interface sites are present, or due to coupling interactions between molecules on non-equivalent sites with short range order. The reduced intensity of bands at 2096 and 2084 cm^{-1} for Ni/sepiolite following an increase in reduction temperature to 873 K (Fig. 6(b)) and a corresponding decrease in dispersion (Table 2) are consistent with this assignment.

Spectra of CO adsorbed on the 773 K reduced (673 K re-reduced) 10% Ni/sepiolite resemble spectra previously reported for lower loaded Ni/sepiolite catalysts [15,16], although for higher loadings (but less than 5% Ni), previously reported spectra are more akin to the 873 K reduced sample used here. Results presented here confirm that the metallic particles formed from a precipitated precursor are morphologically dissimilar to those formed via a route involving impregnation. In a previous study, IR bands due to adsorbed CO were observed at 1995 and 1945 cm^{-1} for samples prepared by impregnation but not those prepared by precipitation [16]. This was attributed to an absence or a physical blocking of (111) faces for the precipitated sample. A more complete study performed here (only selected spectra are shown) involving adsorption and desorption reveals (Fig. 6(c)) that such features are in fact present, but represent a small proportion of the exposed surface. The 1945 cm^{-1} assigned to CO adsorption on 2-fold bridging sites on Ni(111) planes [31], is represented by a weak shoulder on the more intense band at 1956 cm^{-1}. This relationship in intensities is the opposite to that observed for catalysts prepared by impregnation [15,16]. At saturation coverage, the band due to CO on 2-fold bridging sites on Ni(100) appears at higher frequencies than the equivalent carbonyl on the Ni(111) face [31–33] and so the 1956 cm^{-1} band may be attributed to this species. Further evidence for the assignment of exposed (111) planes is the appearance of the 1904 cm^{-1} band following evacuation (Fig. 6(c)) which corresponds with an EELS feature at 1911 cm^{-1} for the same face. While CO on Ni(111) at saturation coverage adsorbs exclusively in the 2-fold bridging mode [31], CO on Ni(100) adsorbs in both bridging and on top modes with the latter giving rise to a band at 2056 cm^{-1} at saturation coverage [33]. The band at 2066 cm^{-1} observed here (Fig. 6(b)) may be attributed to this species, with the ratio of intensities between the 2066/1956 cm^{-1} pair being in agreement with the $\approx$1:2 ratio observed for a pair of bands at 2056/1976 cm^{-1} observed at saturation coverage on the Ni(100) single crystal face [33]. In further agreement and in support of the above assignments, Vasquez et al. [33] showed that decreasing coverage led to the on-top position being favoured at the expense of bridging sites, while here the relative intensities of the 2066/1956 cm^{-1} pair is reversed on evacuation (Fig. 6(c)).

Results presented here are for an average particle size of $\approx$7 nm are roughly in agreement with results of Coulter et al. [32] for model Ni catalysts with a particle size of 8 nm where results indicated the surfaces to consist of mainly (100) and (111) faces. The appearance of additional high frequency bands between 2100–2070 cm^{-1} here which they observed only for 4 nm particles, would indicate that catalysts here have a wider particle size distribution than these model catalysts.

Results here confirm previous reports, that the precipitation of Ni on to sepiolite leads to a particle morphology which favours the exposure of (100) over (111) faces [15,16]. This may be assumed to occur due to growth of a particular precursor orientation followed by direct reduction without nucleation and movement of metal atoms (which would cause clustering and result in random crystal growth). Differences between these

two low index faces in terms of catalytic activity is well known for hydrocarbon reactions with these differences explained in term of steric constraints, electronic differences and differences in terms of carbonaceous laydown [34]. These differences may have been responsible for the dissimilar behaviour observed between catalysts in the hydrogenation of benzene [15] and styrene [16]. It is anticipated that the ability to control the predominant crystal faces exposed during catalysts preparation may be significant in the formation of highly selective catalysts, particularly in the case of reactions showing a degree of site sensitivity.

5. Conclusions

IR and ^{29}Si MAS–NMR confirm that Si–OH groups at the edge sites of silicate layers are consumed when Ni is precipitated on to the sepiolite surface. The formation of nickel silicate rather than hydroxide is distinguished by analysis of the ν_{O-H} and δ_{O-H} modes by IR. The silicate appears to take the form of a 1:1 phyllosilicate (nepouite) rather than a talc (2:1) structure. This precursor–sepiolite interaction is stronger than the interaction between similar species formed over the surface of a silica support. The nickel present is still incompletely reduced after extended treatment in hydrogen at 773 K. Studies of CO adsorption on the reduced catalyst indicate a high concentration of highly dispersed Ni with more open planes and less (111) faces than catalysts of equivalent dispersion formed by other preparation methods. Attempts to completely reduce the nickel by higher temperature treatments result in significant morphological changes.

Acknowledgements

We are grateful to J.LG. Fierro for performing the XPS analysis, M. Faraldos for atomic absorption analysis, J.A. Chudek for guidance with the Solid State NMR facility, Tolsa S.A. Madrid for supplying the sepiolite, The Royal Society (London) for a university research fellowship (J.A.A) and a summer studentship (S.E.F) and the Ministerio de Ciencia y Educación, Spain for the award of a postdoctoral grant (M.G-F).

References

[1] P.N. Rylander, in: J.R. Anderson, M. Boudart (Eds.), Catalysis-Science and Technology, Springer, New York, 1983, vol 4, p. 1.
[2] R.A. Ross, G.D. Martin, W.G. Cook, Ind. Eng. Prod. Res. Dev. 14 (1975) 151.
[3] J.W.E. Coenen, H. Boerma, B.G. Linsen, B. de Vries, in: Sachtler, Shmit, Zwietering (Eds.), Proc. 3rd. Int. Cong. Catal., Amsterdam, 1964, vol. 2, p. 1387.
[4] J.W.E. Coenen, Ind. Eng. Chem. Fundam. 25 (1986) 43.
[5] J.T. Richardson, R.J. Dubus, J. Catal. 54 (1978) 207.
[6] S.-L. Guo, M. Arai, Y. Nishiyama, Appl. Catal. 65 (1990) 31.
[7] R. Fréty, L. Tournayan, M. Primet, G. Bergeret, M. Guenin, J.B. Baumgartner, A. Borgna, J. Chem. Soc. Faraday Trans. 89 (1993) 3313.
[8] K.D. Ghuge, G.P. Babu, J. Catal. 151 (1995) 453.
[9] M. Montes, J.-B. Soupart, M. de Saedeleer, B.K. Hodnett, B. Delmon, J. Chem. Soc. Faraday Trans. 80 (1984) 3221.
[10] L. Zhang, J. Lin, Y. Chen, J. Chem. Soc. Faraday Trans. 88 (1992) 2075.
[11] J. Zielinski, Catal. Lett. 31 (1995) 47.
[12] J.A. van Dillen, J.W. Geus, L.A.M. Hermans, J. van der Miejden, in: G.C. Bond, P.B. Wells, F.C. Tompkins (Eds.), Proc. 6th Int. Cong. Catal., Chemical Society, London, 1976, p. 677.
[13] A. Corma, A. Mifsud, J. Perez Pariente, Ind. Eng. Chem. Res. 27 (1988) 2044.
[14] J.A. Anderson, T. Rodrigo, L. Daza, S. Mendioroz, Langmuir 9 (1993) 2485.
[15] J.A. Anderson, L. Daza, J.G.L. Fierro, M.T. Rodrigo, J. Chem. Soc. Faraday Trans. 89 (1993) 3651.
[16] J.A. Anderson, L. Daza, S. Damyanova, J.G.L. Fierro, M.T. Rodrigo, Appl. Catal. A 113 (1994) 75.
[17] R.F. Rieck, Q.J. Yen, A.T. Bell, J. Catal. 89 (1984) 498.
[18] J.A. Anderson, S.F. Parker, to be published.
[19] P.F. Barron, R.L. Frost, Am. Miner. 70 (1985) 758.
[20] S. Komarneni, C.A. Fyfe, G.J. Kennedy, Clays Clay Miner. 34 (1986) 99.
[21] J.B. d'Espinose de la Caillerie, J.P. Fripiat, Clay Mins. 29 (1994) 313.
[22] J.B. Peri, J. Catal. 8 (1984) 84.
[23] M. Kermarec, J.Y. Carriat, P. Burattin, M. Che, A. Decarreau, J. Phys. Chem. 98 (1994) 12008.
[24] V.C. Farmer in: V.C. Farmer (Ed.), The Infrared Spectra of Minerals, Mineralogical Society, London, 1974, p. 331.
[25] P. Gérard, A.J. Herbillon, Clays Clay Miner. 31 (1983) 143.

[26] O. Clause, M. Kermarec, L. Bonneviot, F. Villain, M. Che, J. Am. Chem. Soc. 114 (1992) 4709.
[27] A.M. Venezia, R. Bertoncello, G. Deganello, Surf. Inter. Anal. 23 (1995) 239.
[28] F.R. Cannings, J. Phys. Chem. 72 (1968) 1072.
[29] M.A. Vicente Rodriguez, J. de, D. Lopez Gonzalez, M.A. Bañares Muñoz, Clay Mins. 29 (1994) 361.
[30] S. Martinez-Ramirez, F. Puertas, M.T. Blanco-Varela, Clay Mins. 31 (1996) 225.
[31] J.C. Bertolini, G. Dalmai-Imelik, J. Rousseau, Surf. Sci. 68 (1977) 539.
[32] K. Coulter, X. Xu, D.W. Goodman, J. Phys. Chem. 98 (1994) 1245.
[33] N. Vasquez Jr., A. Muscat, R.J. Madix, Surf. Sci. 301 (1994) 83.
[34] E. Yagasaki, R.I. Masel, in: J.I. Spivey (Ed.), Specialist Periodical Reports—Catalysis, Royal Society of Chemistry, London, 1994, Vol.11, p. 165.